Quaternary Germanides Formed in Molten Aluminum: $Tb_2NiAl_4Ge_2$ and $Ce_2NiAl_{6-x}Ge_{4-y}$ ($x \sim 0.24$, $y \sim 1.34$)

Brad Sieve, Pantelis N. Trikalitis, and Mercouri G. Kanatzidis*

East Lansing, MI/USA, Michigan State University, Department of Chemistry and Center for Fundamental Materials Research

Received March 25th, 2002.

Dedicated to Professor Welf Bronger on the Occasion of his 70th Birthday

Abstract. The intermetallic phases $Tb_2NiAl_4Ge_2$ and $Ce_2NiAl_{6-x}Ge_{4-y}$ ($x \sim 0.24$, $y \sim 1.34$) were synthesized in molten Al at temperatures below 1000 °C. Both compounds adopt the tetragonal space group *I4/mmm* with cell parameters of $a = 4.1346(2)$ Å $c = 19.3437(7)$ Å for $Tb_2NiAl_4Ge_2$ and $a = 4.1951(9)$ Å and $c = 26.524(7)$ Å for $Ce_2NiAl_{6-x}Ge_{4-y}$. The $Tb_2NiAl_4Ge_2$ structure features $NiAl_4Ge_2$ layers separated by a double layer of rare earth ions. The $Ce_2NiAl_{6-x}Ge_{4-y}$ ($x \sim 0.24$, $y \sim 1.34$) structure also contains the $NiAl_4Ge_2$ layers along with a vacancy defect PbO-type $Al_{2-x}Ge_{2-y}$ layer, and is related to the Ce_2NiGa_{10} structure type. Ordering of vacancies cause the formation of a 3ax3b superstructure in the crystal as seen by electron diffraction experiments. $Tb_2NiAl_4Ge_2$ exhibits Curie-Weiss paramagnetic behavior with an antiferromagnetic transition observed at ~20 K. $Ce_2NiAl_{6-x}Ge_{4-y}$ shows a much more complex magnetic behavior possibly due to temperature induced variation in the valency of the Ce atoms.

Keywords: Germanides (quaternary); Rare earth elements; Nickel; Aluminium; Crystal structure; Magnetic properties

In flüssigem Aluminium gebildete quaternäre Germanide: $Tb_2NiAl_4Ge_2$ und $Ce_2NiAl_{6-x}Ge_{4-y}$ ($x \sim 0.24$, $y \sim 1.34$)

Inhaltsübersicht. Die intermetallischen Phasen $Tb_2NiAl_4Ge_2$ und $Ce_2NiAl_{6-x}Ge_{4-y}$ ($x \sim 0.24$, $y \sim 1.34$) wurden in geschmolzenem Al bei Temperaturen unter 1000 °C synthetisiert. Beide Verbindungen haben die tetragonale Raumgruppe *I4/mmm* mit den Gitterparametern $a = 4{,}134(2)$ Å, $c = 19{,}3437(7)$ Å für $Tb_2NiAl_4Ge_2$ und $a = 4{,}1951(9)$ Å und $c = 26{,}524(7)$ Å für $Ce_2NiAl_{6-x}Ge_{4-y}$. Die Struktur von $Tb_2NiAl_4Ge_2$ wird aus $NiAl_4Ge_2$-Schichten, die durch eine Doppelschicht von Seltenerdionen getrennt sind, aufgebaut. Die $Ce_2NiAl_{6-x}Ge_{4-y}$ ($x \sim 0.24$, $y \sim 1.34$)-Struktur enthält ebenfalls die $NiAl_4Ge_2$-Schichten mit einer $Al_{2-x}Ge_{2-y}$-Schicht vom Leerstellendefekt-PbO-Typ und ist mit dem Ce_2NiGa_{10}-Strukturtyp verwandt. Die Ordnung der Leerstellen bewirkt die Bildung einer 3a×3b-Superstruktur im Kristall, wie aus Elektronenbeugungsversuchen zu ersehen ist. $Tb_2NiAl_4Ge_2$ zeigt Curie-Weiss paramagnetisches Verhalten mit einem antiferromagnetischen Übergang bei ≈20 K. $Ce_2NiAl_{6-x}Ge_{4-x}$ zeigt ein sehr viel komplexeres magnetisches Verhalten, wahrscheinlich aufgrund von temperaturinduzierten Änderung der Valenz des Ce-Atoms.

Introduction

The use of metal fluxes in exploratory synthesis presents significant synthetic advantages such as solution-like conditions, lower reaction temperatures, facile crystal growth, and "freeing" the reaction system to find its way to the final product under the prevailing experimental conditions [1]. This is in stark contrast to direct solid state reactions that involve combination of reactants in stoichometric ratios at very high temperatures, where often only polycrystalline powders are obtained. Molten metals can provide an excellent medium for the exploratory synthesis of complex phases such as tetrelide compounds (i.e. Si and Ge) from liquid Al and Ga. This approach generated many new Al containing compounds including $Sm_2Ni(Si_{1-x},Ni_x)Al_4Si_6$ [2], $RENiAl_4Ge_2$ (RE = Sm, Tb, Y) [3], $RE_2Fe(Fe,Si)Al_3Si_4$ (RE = Ce, Pr, Nd, Sm) [4], $REFe_4Al_9Si_6$ (RE = Tb, Er) [5], $RE_8Ru_{12}Al_{49}Si_9(Al_xSi_{12-x})$ (RE = Sm and Pr) [6] and $RE_2Al_3Si_2$ (RE = Ho, Er, Tm) [1a]. In addition to being of basic scientific interest complex intermetallics of Al are of interest to applied metallurgy due to their compositional relationships to aluminum matrix composites [7]. Many Al matrix composites contain other elements that react and form ternary or quaternary aluminide phases within the Al matrix, either during the material's initial preparation or over time with use. These newly formed phases may be responsible for the beneficial properties of the alloys or may contribute to the alloy's eventual failure. Detailed knowledge of these minor but important phases and their behavior can therefore be critical in understanding and designing better materials for the future. An example of the importance of complex multinary compounds forming in Al alloys is $Cu_2Mg_8Al_5Si_6$ which has been shown to significantly increase the matrix's strength without increasing its overall weight [8]. Examples of Ge phase precipitation are

* Prof. Dr. Mercouri G. Kanatzidis
Michigan State University, Department of Chemistry and Center for Fundamental Materials Research
East Lansing, MI 48824-1322 / USA
E-Mail: kanatzid@cem.msu.edu

  0044−2313/02/628/1568−1574 $ 20.00+.50/0 Z. Anorg. Allg. Chem. **2002**, *628*, 1568−1574

much rarer though several systems are now being studied including binary Ni/Ge phases [9], Si/Ge solid precipitant in Al matrixes [10], and Mg/Ge phases forming in Al/Cu/Mg/Si/Ge systems [11]. In this paper the reactivity of Ge was explored and two new Al containing quaternary compounds, $Tb_2NiAl_4Ge_2$ and $Ce_2NiAl_{6-x}Ge_{4-y}$ ($x \sim 0.24$, $y \sim 1.34$), are presented each synthesized in molten Al below 1000 °C. Noteworthy is the highly stable building unit $NiAl_4Ge_2$ observed in the compounds. Along with a detailed discussion of the structures magnetic data are also reported.

Experimental Section

Synthesis

$Tb_2NiAl_4Ge_2$. Method 1: In a N_2 filled glove box Tb (Cerac Inc., −40 mesh, 99.99%), Ni (Aldrich, powder, 99.99%), Al (Cerac Inc., −20 mesh, 99.5%), and Ge (Cerac Inc., powder, 99.999%) powders were mixed in a 2:1:10:2 ratio. The mixture was then placed into an alumina crucible and sealed within a fused silica tube under vacuum ($<1x10^{-4}$ Torr). The tubes were heated to 1000 °C over a period of 24 hours and kept there for 48 hours. They were then slowly cooled to 500° C over 48 hours followed by cooling to 50° C in 12 hours. The alumina tubes were removed from the silica and submerged in 5M NaOH for 24 hours to remove the excess Al matrix. This procedure yielded two types of products, silvery plate-like crystals and black microcrystalline powder both of which were shown to be the same phase, by comparison of experimental powder patterns to patterns generated from the solved crystal structure. This reaction shows yields greater than 85%, based on Tb.

Method 2: In a N_2 filled glove box Tb (Cerac Inc., −40 mesh, 99.99%), Ni (Aldrich, powder, 99.99%), Al (Cerac Inc., −20 mesh, 99.5%), and Ge (Cerac Inc., powder, 99.999%) powders were mixed in a 2:1:10:2 ratio. This mixture was pressed and loaded into an arc wielder and melted, under an Ar atmosphere, for approximately 30 seconds until a good melt was observed. The samples were then flipped and remelted several times to ensure homogeneity in the overall sample. After cooling, crystals were observed on the surface of the ingot imbedded in the excess Al. The excess Al matrix was removed by submersion in 5M NaOH for 24 hours. After the isolation was complete an X-ray powder diffraction pattern was recorded which matched well with the calculated pattern. Based on the Tb yields for this reaction were on the order of 80%. Reaction attempts without excess Al did not produce pure product but instead mixtures of phases including $TbNiAl_4Ge_2$ [3] and $Tb_2NiAl_4Ge_2$.

$Ce_2NiAl_{6-x}Ge_{4-y}$ ($x \sim 0.24$, $y \sim 1.34$). In a N_2 filled glove box Ce (Cerac Inc., −40 mesh, 99.99%), Ni (Aldrich, powder, 99.99%), Al (Cerac Inc., −20 mesh, 99.5%), and Ge (Cerac Inc., powder, 99.999%) powders were mixed in a 1:1:30:1 ratio. The mixture was then placed into an alumina crucible and sealed within a fused silica tube under a vacuum ($<1x10^{-4}$ Torr). The tubes were heated to 850 °C over a period of 20 hours and kept there for 96 hours. They were then slowly cooled to 500 °C over 72 hours and to 50° C in 12 hours. The alumina tubes were removed from the silica and submerged in 5M NaOH for 24 hours. This dissolved the excess Al and yielded both plate-like crystal and black microcrystalline power. Both products were identified as a single phase by comparison of experimental powder patterns to those generated from the solved crystal structure. This reaction shows yields of ~80% based on Ge.

EDS analysis

Quantitative microprobe analysis of the two compounds was performed with a JEOL JSM-6400 Scanning Electron Microscope (SEM) equipped with Noran Energy Dispersive Spectroscopy (EDS) detector. Data were acquired using an accelerating voltage of 25 kV and 100 sec accumulation time. Standards where recorded under the same experimental conditions to yield correction factors. After calibration the Tb compound gave an elemental ratio of 1.99 Tb: 1 Ni: 4.01 Al: 1.95 Ge, well within experimental errors from the actual formula. For $Ce_2NiAl_{6-x}Ge_{4-y}$ ($x \sim 0.24$, $y \sim 1.34$) the elemental analysis yielded a formula of $Ce_2Ni_{1.06}Al_{6.58}Ge_{2.30}$. This ratio is very close to the final crystallographically refined elemental ratios in the respect to the Ce, Ge, and Ni, however Al exhibited an error of 10% over the actual formula of the compound. Crystals selected from different preparation methods did not show significant differences in elemental ratio.

Electron Diffraction Studies (TEM)

Electron crystallographic studies were carried out on a JEOL 100CX transmission electron microscope (TEM) equipped with a CeB_6 filament and an accelerating voltage of 120 kV. The samples were gently ground into a fine powder and the specimens were prepared by dipping a carbon coated copper grid into the microcrystalline powder. The samples showed no decomposition under the electron beam.

X-ray Crystallography

Single crystal X-ray diffraction data for $Tb_2NiAl_4Ge_2$ and $Ce_2NiAl_{6-x}Ge_{4-y}$ ($x \sim 0.24$, $y \sim 1.34$) were collected at 298 K on a Siemens Platform CCD diffractometer using Mo Kα ($\lambda = 0.71069$ Å) radiation. The SMART software [12] was used for the data acquisition and the program SAINT [13] was used for the data extraction and reduction. An empirical absorption correction using SADABS [14] was applied to the $Tb_2NiAl_4Ge_2$ data while a face indexed absorption correction was performed on the data of $Ce_2NiAl_{6-x}Ge_{4-y}$ utilizing the SHELXL software [15]. These structures were solved and refined with the SHELXL package of programs. The crystallographic and refinement details are listed in Table 1. The fractional atomic positions, displacement parameters (U values) and selected bond distances are listed in Tables 2−5.

Magnetic Susceptibility Measurements

Magnetic susceptibility for $Tb_2NiAl_4Ge_2$ and $Ce_2NiAl_{6-x}Ge_{4-y}$ ($x \sim 0.24$, $y \sim 1.34$) was measured as a function of both temperature and field using a MPMS Quantum Design SQUID magnetometer. Single crystal measurements, both parallel and perpendicular to the c-axis, were conducted for $Tb_2NiAl_4Ge_2$ while powder samples were used in measuring $Ce_2NiAl_{6-x}Ge_{4-y}$. An initial study of field dependence was conducted to find a suitable field for the variable temperature studies. These measurements on all samples were then conducted under increasing temperature using a 500 G applied field. Field dependent measurements, conducted at 5K, were carried out between ±55000 G for the Ce analog and 0 to 55000 G for $Tb_2NiAl_4Ge_2$ single crystals. A diamagnetic correction was applied to the data to account for core diamagnetism. No correction was made for the sample container however as the measured moment was well over an order of magnitude smaller then the sample signal itself.

Table 1 Crystallographic data for $Tb_2NiAl_4Ge_2$ and $Ce_2NiAl_{6-x}Ge_{4-y}$ (y ~ 0.24, x ~ 1.34)

Formula	$Tb_2NiAl_4Ge_2$	$Ce_2NiAl_{5.77}Ge_{2.64}$
Formula weight	629.63	686.26
Temperature/K	298	298
Wavelength/Å	0.71073	0.71073
Space group	I4/mmm (#139)	I4/mmm (#139)
Crystal size/mm	0.12 x 0.15 x 0.24	0.01 x 0.16 x 0.20
Unit cell dimensions/Å	a = 4.1346(2)	a = 4.1951(9)
	c = 19.3437(7)	c = 26.524(7)
Volume/Å^3	330.68(3)	466.8(2)
μ/mm^{-1}	18.028	13.577
Θ range/°	2.11 to 28.24	1.54 to 28.65
Index ranges	−5<h<5	−5<h<5
	−5<k<5	−5<k<5
	−25<l<20	−33<l<35
Reflections Collected	1413	2307
Unique Reflections	158 [R(int) = 0.0683]	221 [R(int) = 0.0324]
Data/restraints/parameters	158/0/14	221/0/24
Goodness-of-fit on F_o^2	1.093	1.205
Final R indices [I>2σ(I)]	R1 = 0.0252, wR2 = 0.0698	R1 = 0.0382, wR2 = 0.1065
R indices (all data)	R1 = 0.0266, wR2 = 0.0703	R1 = 0.0382, wR2 = 0.1065
Largest diff. peak and hole/(e/Å^3)	1.819 and −2.182	1.714 and −2.999

Table 2 Atomic coordinates (x 10^4) and anisotropic displacement parameters (A^2 x 10^3) for $Tb_2NiAl_4Ge_2$ (y = 0) (U23 = U13 = U12 = 0).

	Wykoff Position	x	z	U11	U22	U33
Tb	4e	0	1864(1)	3(1)	3(1)	6(1)
Ge	4e	0	3383(1)	3(1)	3(1)	6(1)
Ni	2a	0	0	3(1)	3(1)	3(1)
Al	8g	−5000	672(2)	3(1)	7(2)	8(2)

The anisotropic displacement factor exponent takes the form: $-2\pi^2$ [h^2 a*^{2} U11 + ... + 2 h k a* b* U12]

Table 3 Selected bond lengths/Å for $Tb_2NiAl_4Ge_2$.

Tb-Ge	2.937(2)
Tb-Al	3.097(3)
Tb-Tb	3.821(1)
Ge-Al	2.760(2)
Ge-Tb	2.9623(4)
Ni-Al	2.442(2)
Al-Al	2.599(6)
Al-Al	2.9236(1)

Table 4 Atomic coordinates (x 10^4) and anisotropic displacement parameters (A^2 x 10^3) for and $Ce_2NiAl_{6-x}Ge_{4-y}$ (x ~ 0.24, y ~ 1.34) (U23 = U13 = U12 = 0).

	Wykoff Position	x	y	z	U11	U22	U33	occupancy
Ce	4e	0	0	1481(1)	10(1)	10(1)	10(1)	1
Ni	2a	0	0	0	8(1)	8(1)	13(2)	1
Ge(1)	4e	5000	5000	1119(1)	17(1)	17(1)	23(1)	1
Al(1)	8g	5000	0	491(1)	9(2)	10(2)	10(2)	1
Ge(2)	4d	5000	0	2500	53(5)	53(5)	28(5)	0.32
Al(2)*	16n	121(4)	0	2903(5)	40(11)	14(7)	24(6)	0.22

The anisotropic displacement factor exponent takes the form $-2\pi^2$ [h^2 a*^{2} U11 + ... + 2 h k a* b* U12]
* Al(2) has U13 = −19(6)

Table 5 Selected bond lengths/Å for $Ce_2NiAl_{6-x}Ge_{4-y}$ (x ~ 0.24, y ~ 1.34).

Ce-Al(2)	3.10(1)
Al(1)-Ce	3.361(3)
Ce-Ge(1)	3.118(1)
Ni-Al(1)	2.469(2)
Ge(1)-Al(6)	2.64(1)
Ge(1)-Al(1)	2.678(3)
Ge(1)-Ce	3.118(1)
Al(1)-Al(1)	2.9664(6)
Ge(2)-Al(2)	1.92(2)
Ge(2)-Al(2)	2.408(6)
Al(2)-Al(2)	0.72(2)
Al(2)-Al(2)	1.02(3)
Al(2)-Ge(2)	2.82(2)

Results and Discussion

Synthesis

The combination of rare earth elements Ce and Tb, Ni, and Ge in excess Al conveniently yielded large crystals of the title quaternary compounds. Molten Al is an excellent reaction media since it allows the reaction solution to contain large amounts of dissolved Ge in a very reactive state, due to the absence of binary Al/Ge phase formation. This high concentration of Ge then creates an excellent reaction environment with other elements, present in the solution, even if only in small amounts. Both title compounds form large (>1mm per side) shiny silver crystals with plate-like morphologies readily from such mixtures.

Structure Description

$Tb_2NiAl_4Ge_2$ crystallizes in the space group *I4/mmm* (#139) with the structure shown in Figure 1. It is best described as $NiAl_4Ge_2$ slabs alternating with a bilayer of rare earth atoms. The $NiAl_4Ge_2$ unit is a very stable structural unit, related to the antiflourite structure type, and is seen

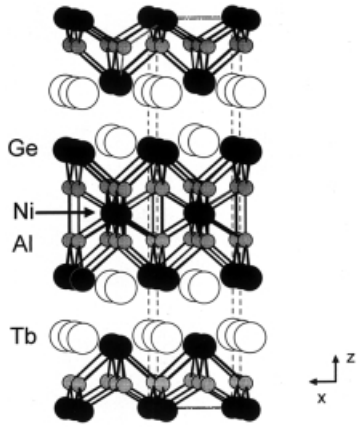

Figure 1 Structure of $Tb_2NiAl_4Ge_2$ viewed down the *b* axis.

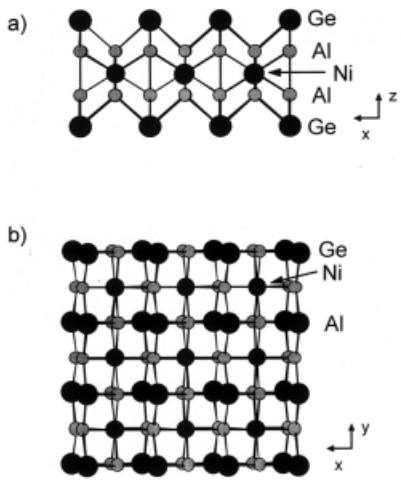

Figure 2 Views of the $NiAl_4Ge_2$ layer viewed down (a) the *b* axis and (b) the *c* axis.

in many intermetallic compounds such as $LaGa_6Ni_{1-x}$ [16], $Sm_2Ni(Si_{1-x},Ni_x)Al_4Si_6$ [2] and $LaNi_{1+x}Al_4Si_{2-x}$ [17]. The slab is five atomic layers thick with the stacking sequence Ge/Al/Ni/Al/Ge, see Figure 2. The Ni atoms occupy the center of slightly distorted Al cubes to form $NiAl_8$ units. Each of these are then merged with four other $NiAl_8$ units, sharing edges, to form an infinite layer with one half of the cubes filled with a Ni center. The Ge atoms then cap above and below the Al_8 cubes not centered by Ni atoms.

The Ge atoms themselves are in a four coordinate square pyramidal $GeAl_4$ arrangement that requires all Ge-Al bonds to be pointed towards the center of the $NiAl_4Ge_2$ layer, Figure 3a. The Al atoms in the layer exhibit a five coordinate environment which can be described as a capped tetrahedral arrangement namely they are bonded to 2 Ni atoms, 2 Ge atoms and one capping Al atom, see Figure 3b. The Al atoms lie on a plane and define a perfect square net. The Al-Al distance in the plane 2.9236(1) Å, slightly longer than that normally considered a strong bonding interaction, however weak interactions are likely present. The

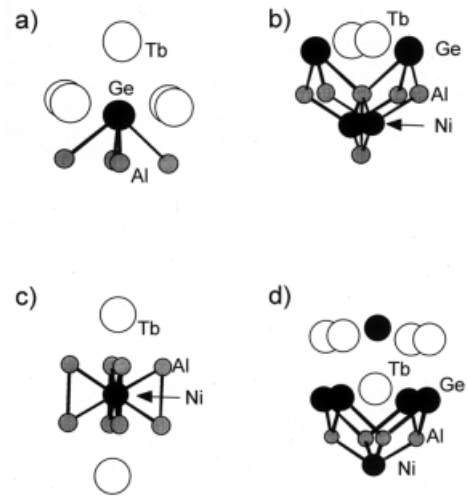

Figure 3 Local coordination environments of individual atomic positions in $Tb_2NiAl_4Ge_2$.

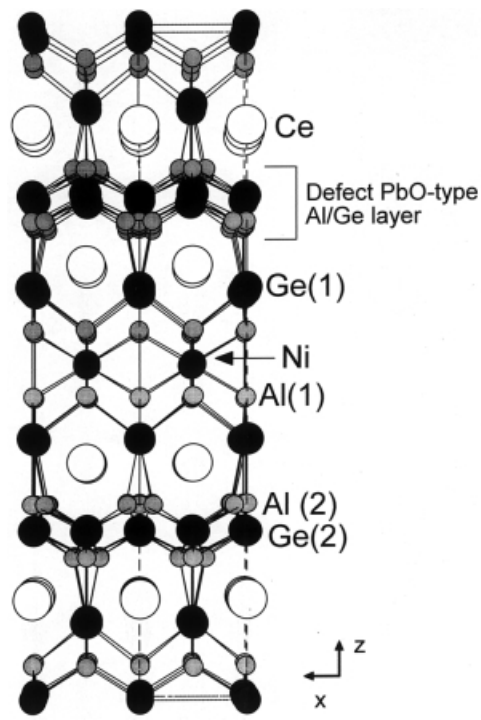

Figure 4 Structure of $Ce_2NiAl_{6-x}Ge_{4-x}$ (y ~ 0.24, x ~ 1.34) viewed down the *b* axis.

nickel atoms exhibit a square prismatic (nearly cubic) environment of 8 Al atoms, Figure 3c. The Ni-RE distance in this compound is 3.606 Å. The rare earth ion in the structure exhibits bonding (defined as <3.5 Å) to 4 Al atoms and 5 Ge atoms in a 9 coordinate environment.

The compound $Ce_2NiAl_{6-x}Ge_{4-y}$ (x ~ 0.24, y ~ 1.34) is of the Ce_2NiGa_{10} structure type [18] with substantial structural deviations, see Figure 4. The structure consists of alternating RE layers (A), layers of $NiAl_4Ge_2$ (B) (same as

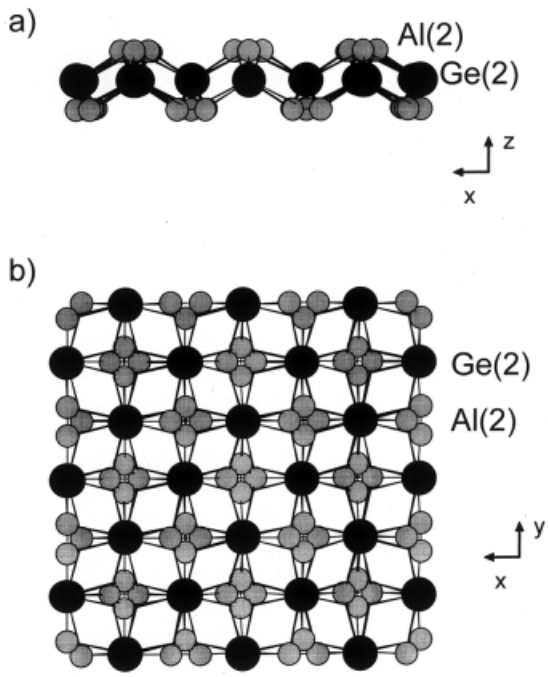

Figure 5 Views of the heavily vacant $Al_{2-x}Ge_{2-y}$ ($x \sim 0.24$, $y \sim 1.34$) layer viewed down (a) the *b* axis and (b) the *c* axis. The disordered Al atoms are shown.

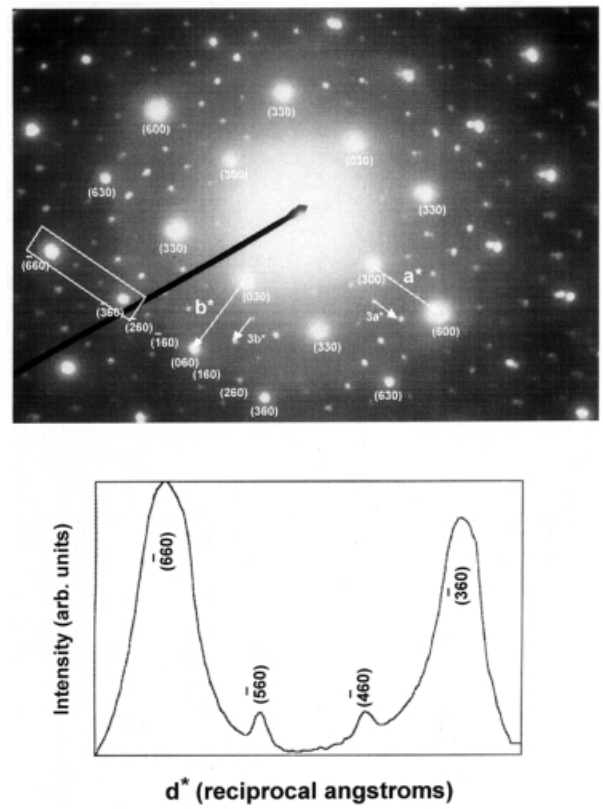

Figure 6 (a) Selected area diffraction pattern of $Ce_2NiAl_{6-x}Ge_{4-y}$, viewed down the c axis (hk0 zone), showing the *3a* x *3b* supercell and (b) one-dimensional peak intensity profile from the boxed area indicated in the pattern clearly showing the weak *(5̄60)* and *(4̄60)* commensurate supercell reflections.

those described above for $Tb_2NiAl_4Ge_2$) and $Al_{2-x}Ge_{2-y}$ layers (C) which adopt a defect PbO-type structure. These layers alternate in a ABACABA fashion along the *c* axis of the unit cell. The difference from the Ce_2NiGa_{10} structure type is exhibited in the PbO layers. The parent compound exhibits ideal and complete Ga layers of PbO-type while in $Ce_2NiAl_{6-x}Ge_{4-y}$ these layers are now AlGe with vacancies on the Ge and Al positions and a displacement of Al atoms off the 4e special position (site symmetry 4mm), see Figure 5. The shifting of the Al atoms off the 4e position shifting to position 16n creating four closely lying symmetry related atoms with a short Al-Al distance of 0.72 Å. For this quartet, three bond distances to the neighboring Ge atom (2.817 Å, 2.408 Å, and 2.408 Å) are reasonable whereas the fourth is too short to be realistic at 1.92(2) Å. The occupancy of this Al position refined to 22% of the total full position suggesting that it is present approximately $1/4^{th}$ of the time as would be expected for a simple displacement of a single Al atom from a special to a general position. At the same time the occupancy of the Ge(2) atoms in the layer refined to 32 %. The vacancies in the Ge layer alleviates the need for the short 1.92(2) Å distances, which are only apparent and the result of averaging the structure to a *I4/mmm* unit cell. The rare earth ions occupy high coordination sites.

The observed vacancies and disorder raises the question of possible long range ordering in the Al/Ge layer and the existence of a larger structural supercell. To examine this, electron diffraction experiments were conducted on samples of $Ce_2NiAl_{6-x}Ge_{4-y}$. Supercell peaks are indeed seen in selected area electron diffraction patterns indicating long range ordering in the structure, see Figure 6. The observed diffraction pattern be can indexed to a commensurate *3a x 3b* supercell with lattice constants of $a = 12.58$ Å and $b = 12.58$ Å. We have no information on ordering along the *c* axis, as electron diffraction examining this axis was very difficult due to the thin plate morphology of the crystals. A satisfactory X-ray refinement based on this larger cell could not be reached, however, due to the very low inherent reflection intensity exhibited by the supercell reflections.

Magnetic Measurements

Magnetic susceptibility data for $Tb_2NiAl_4Ge_2$, measured on a single crystal, showed an antiferromagnetic transition with a Neel temperature of ~20 K for both crystal orientations in relation to the applied field, see Figure 7a. Above this temperature both orientations exhibit Curie-Weiss behavior as shown in the inlay of Figure 7a. With the crystallographic c-axis oriented along the applied field a Weiss constant, θ, of −92.78 K is found. The μ_{eff}, calculated from the Curie-Weiss behavior was 9.96 μ_B per Tb atom. With the field oriented perpendicular to the *c*-axis, i.e. in the *ab*-plane, the compound exhibits a μ_{eff} of 9.77 μ_B and a θ of

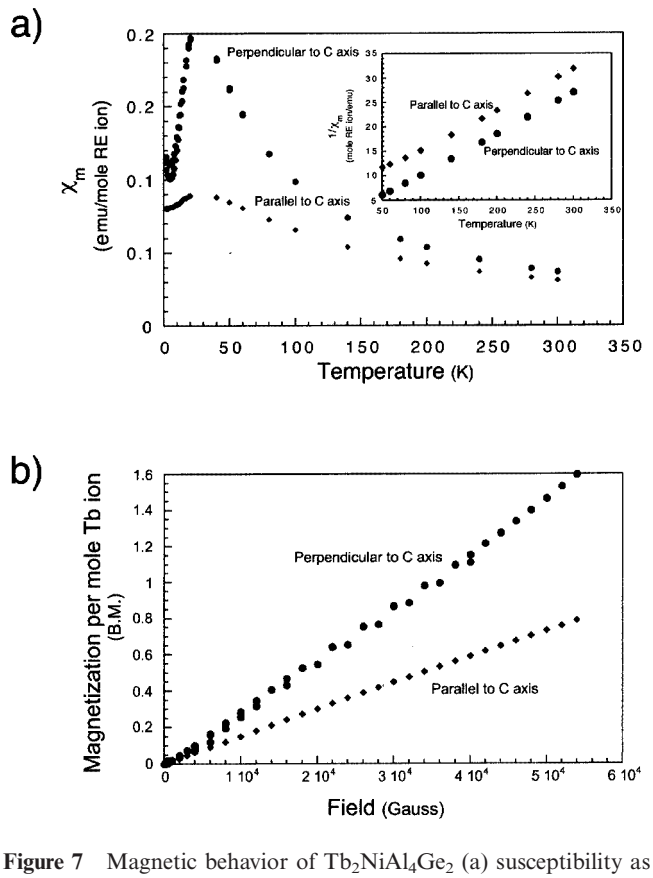

Figure 7 Magnetic behavior of $Tb_2NiAl_4Ge_2$ (a) susceptibility as a function of temperature (inset shows the inverse response) and (b) magnetization as a function of field.

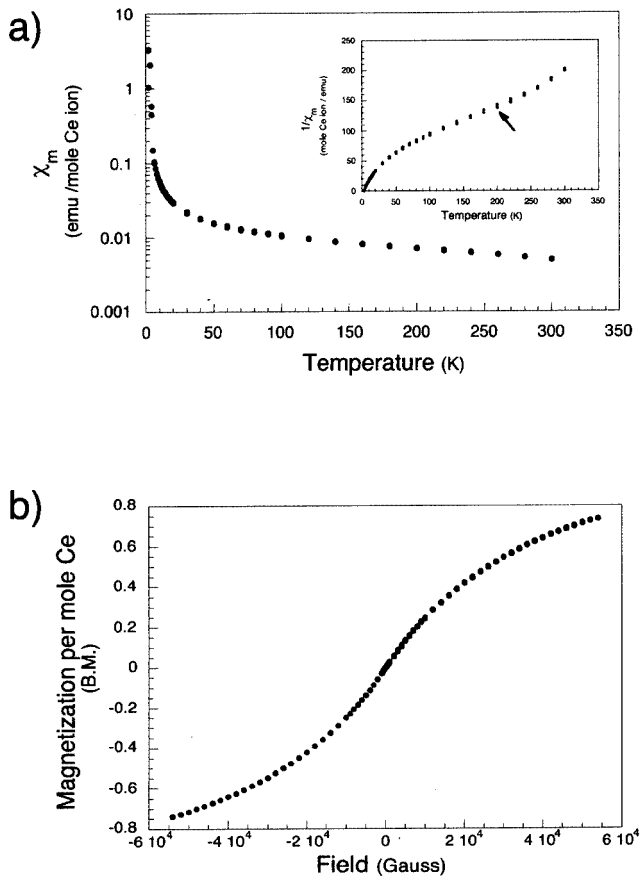

Figure 8 Magnetic behavior of $Ce_2NiAl_{6-x}Ge_{4-y}$ ($x \sim 0.24$, $y \sim 1.34$) (a) susceptibility as a function of temperature (inset shows the inverse response) and (b) magnetization as a function of field. Note the arrow in inset marks the slope change at high temperatures.

−21.6 K. The μ_{eff} values are very close to the theoretical magnetic moment for Tb^{3+} of 9.72 μ_B [19], indicating that Ni is diamagnetic as is the case in other transition metal aluminum compounds [2, 3]. Well below the transition temperature, at ~5 K, the magnetization curve shows a linear increase with increasing field up to 55,000 G with no indications of magnetic saturation, see Figure 7b.

Samples of $Ce_2NiAl_{6-x}Ge_{4-y}$ ($x \sim 0.24$, $y \sim 1.34$) exhibit more complex magnetic properties with no Curie-Weiss behavior at any temperature. At low temperatures a ferromagnetic transition was observed at ~4K, while at higher temperatures the compound showed a weak transition, at about 200K (indicated by an inflection point), which significantly decreases the magnetization with rising temperatures. This behavior is expressed by the dramatic change in the slope of the inverse susceptibility plot, shown by arrow in the Figure 8a inset, and may be due to valence fluctuations in Ce over the measured temperature range [20]. The Ce atom formal valency in this compound however is likely 3+. When the field dependence was studied at 5 K a gradual saturation of the moment is seen with increasing fields with a lack of hysteresis, see Figure 8b. Complete magnetic saturation did not occur however before 55000 G.

Concluding Remarks

Because of its ability to dissolve large amounts of Ge, liquid Al is an excellent reactive solvent for the formation of complex $Tb_2NiAl_4Ge_2$ and $Ce_2NiAl_{6-x}Ge_{4-y}$. These phases form large single crystals at temperatures well below those needed for traditional synthesis. Of particular interest is the observation of the $NiAl_4Ge_2$ building block in both the systems and its occurrence in many intermetallic compounds. This underscores its exceptional stability, in a variety of environments and synthetic conditions, suggesting it should be viewed as a basic building block. Finally the Tb in $Tb_2NiAl_4Ge_2$ exhibits a 3+ oxidation state while the Ce atom in $Ce_2NiAl_{6-x}Ge_{4-y}$ may undergo a possible valence fluctuations with changes in temperature.

Acknowledgments: Financial support from the Department of Energy (Grant No. DE-FG02-99ER45793) is gratefully acknowledged. This work made use of the SEM and TEM facilities of the Center for Advanced Microscopy at Michigan State University. We would also like to extend a special thanks to *Prof. Canfield* at Iowa State University for growing crystals of the $Tb_2NiAl_4Ge_2$ phase.

References

[1] (a) X. Z. Chen, B. Sieve, R. Henning, A. J. Schultz, P. Brazis, C. R. Kannewurf, J. A. Cowen, R. Crosby, M. G. Kanatzidis, *Angew. Chem. Int. Ed.* **1999,** *38*, 693−696. (b) S. Okada, Y. Yu, T. Lundström, K. Kudou, T. Tanaka *Jpn. J. Appl. Phys.* **1996**, *35*, 4718−4723. (c) S. Nieman, W. Jeitschko, *J. Solid State Chem*. **1995**, *116*, 131−135. (d) S. Nieman, W. Jeitschko, *J. Alloys Comp.* **1995**, *221*, 235−239.

[2] X. Z. Chen, S. Sportouch, B. Sieve, P. Brazis, C. R. Kannewurf, J. A. Cowen, R. Patschke, M. G. Kanatzidis, *Chem. Mater*. **1998**, *10*, 3202−3211.

[3] B. Sieve, X. Z. Chen, J. A. Cowen, P. Larson, S. D. Mahanti, M. G. Kanatzidis, *Chem Mater.* **1999**, *11*, 2451−2455.

[4] B. Sieve, S. Sportouch, X. Z. Chen, J. A. Cowan, P. Brazis, CR. Kannewurf, V. Papaefthymiou, M. G. Kanatzidis, *Chem. Mater.* **2001**, *13*, 273−283.

[5] B. Sieve, R. Henning, T. Bakas, A. J. Schultz, M. G. Kanatzidis, work in progress.

[6] B. Sieve, X. Z. Chen, R. Henning, P. Brazis, C. R. Kannewurf, J. A. Schultz, M. G. Kanatzidis, *J. Am. Chem. Soc.* **2001**, *29*, 7040−7047.

[7] S. Suresh, A. Mortensen, A. Needleman, *Fundamentals of Metal-Matrix Composites*, Butterworth-Heinemann, Boston, 1993.

[8] (a) G. C. Weatherly, A. Perovic, N. K. Mukhopadhyay, D. J. Lloyd, D. D. Perovic, *Metall. Mater. Trans. A*, **2001**, *32A*, 213−218; (b) K. Matsuda, Y. Uetani, T. Sato, S. Ikeno, *Metall. Mater. Trans. A*, **2001**, *32A*, 1293−1299.

[9] Y. Jin, M. C. Chaturvedi, *Modern Physics Letters B*, **1996**, *10*, 1111−1112.

[10] D. Miltin, V. Radmilovic, D. Dahmen, J. W. Morris, Jr., *Metall. Mater. Trans. A*, **2001**, *32A*, 197−199.

[11] S. P. Ringer, S. P. Swenser, B. C. Muddle, I. J. Polmear, T. Sakurai, *Mater. Sci. Forum* **1996**, *217*, 689−694

[12] SMART. Data Collection Software for the SMART System. Siemens Analytical X-Ray Instruments Inc., 1995.

[13] SAINT. Data Processing Software for SMART System. Siemens Analytical X-Ray Instruments Inc., 1995.

[14] G. M. Sheldrick, University of Göttingen, Germany, manuscript to be published.

[15] G. M. Sheldrick, *SHELXL. Structural Determination Programs*, Version 5.0; Siemans Analytical X-Ray Instruments Inc.: Madison, WI, 1995.

[16] Yu. N. Grin, Ya. P. Yarmolyuk, I. V. Rozhdestvenskaya, E. I. Gladyshevskii, *Sov. Phys. Crystallogr.* **1982**, *27*, 418−419.

[17] B. Sieve, M. G. Kanatzidis, to be published.

[18] Ya. P. Yarmolyuk, Yu. N. Grin, I. V. Rozhdestvenskaya, O. A. Usov, A. M. Kuz'min, V. A. Bruskov, E. I. Gladyshevskii, *Sov. Phys. Crystallogr.* **1982**, *27*, 599−600.

[19] E. A. Bourdreaux, L. N. Mulay, in *Theory and Applications of Molecular Paramagnetism*, John Wiley and Sons, New York **1976**.

[20] (a) G. H. Kwei, J. M. Lawrence, P. C. Canfield, *Phys. Rev. B*, **1994**, *49*, 1408−1410; (b) Thermopower measurements were then conducted to probe possible Ce valence fluctuations. The thermopower values ranged from ±5 μV/K, in the temperature range of 50−300 K and suggest metallic behavior. However they provided no information about any of valence fluctuations in the Ce atoms.